

See discussions, stats, and author profiles for this publication at: <https://www.researchgate.net/publication/260589392>

# EMI filter design: Part II: Measurement of noise source impedances

Article in IEEE Electromagnetic Compatibility Magazine · March 2012

DOI: 10.1109/EMEC.2012.6244944

---

CITATIONS

9

---

READS

2,695

1 author:



V. Tarateeraseth

Srinakharinwirot University

57 PUBLICATIONS 391 CITATIONS

SEE PROFILE

Some of the authors of this publication are also working on these related projects:



Conducted Emission Characteristics of an Active Snubber Boost Converter [View project](#)

# EMI Filter Design

## Part II: Measurement of Noise Source Impedances

**Vuttipon Tarateeraseth, Member, IEEE, Department of Electrical Engineering, Srinakharinwirot**

**University, Thailand**

**E-mail: vuttipon@ieee.org**

**Abstract** – In the first part of the EMI filter design series, the conducted EMI generation mechanism was explained. In this second part, a method on the measurement of noise source impedance of SMPS will be described. The proposed measurement method allows accurate extraction of the common-mode and differential-mode equivalent noise source impedances of a SMPS under its actual operating conditions.

### I. Introduction

A built-in power line electromagnetic interference (EMI) filter is a part of a switched-mode power supply (SMPS) to limit conducted EMI in the frequency range up to 30 MHz in order to comply with the international EMI regulatory requirements [1], [2]. Unlike the filters used in communications and microwave applications, where the source and the termination impedances are well-defined as  $50\ \Omega$ , the actual noise source and the termination impedances of an EMI filter in a SMPS are far from  $50\ \Omega$  [3]. In the standard conducted EMI measurement setup, the SMPS is powered through the line impedance stabilization network (LISN) whose impedance is well-defined [4]. Unfortunately, the noise source impedance of a SMPS varies with several parameters such as converter topology, power rating, component parasitic elements and board layout [5]. For example, the DM noise source impedance is strongly influenced by the reverse recovery phenomena of the diode rectifier [6], the equivalent series resistance (ESR) and the equivalent series inductance (ESL) of the bulk capacitor [7]. As for the CM noise source impedance, the deciding components are the parasitic capacitance between the switching device and its heat-sink and the parasitic capacitance between the board and the chassis [2], [8]. Hence, designing an EMI filter for a SMPS by assuming  $50\ \Omega$  noise source and termination impedances will lead to non-optimal EMI suppression performance from the filter.

Some progress has been made to measure the DM and CM noise source impedances of a SMPS. Firstly, the resonance method was developed to estimate the noise source impedance of a SMPS by making a simplifying assumption that the noise source is a simple Norton equivalent circuit of a current source with parallel resistive and capacitive elements [9]. By terminating at the AC power input of the SMPS with a resonating inductor, the noise source impedance can be estimated [10]. However, the process to select and to tune the resonating inductor for resonance can be tedious and cumbersome. Also, when frequency increases, the parasitic effects of the non-ideal reactive components become significant

and the circuit topology based on which the resonance method is developed is no longer valid. This simplistic approach provides only a very rough estimate of the noise source equivalent circuit model.

Some time ago, the insertion loss method was introduced to measure the DM and CM noise source impedances of a SMPS [11]. This method requires some prior conditions to be fulfilled. For example, the impedances of the inserted components must be much larger or smaller than the noise source impedances [12]. Hence, the accuracy deteriorates if these conditions are not met. Moreover, it only provides the magnitude information of the noise source impedance and the phase information can only be estimated with a complicated Hilbert transform process.

Recently, a two-probe approach to measure the DM and CM noise source impedances of a SMPS was developed [13]. An injecting probe, a sensing probe and some coupling capacitors are used in the measurement setup. In order to measure the DM and CM noise source impedances with reasonable accuracy, careful choices of the DM and CM chokes are necessary to provide very good RF isolation between the SMPS and the LISN. Moreover, special attention is needed to ascertain that the DM and the CM chokes are not saturated for the SMPS of higher power rating. Again, this method focuses on extracting the magnitude information of the noise source impedance only.

In view of the limitations of the previously discussed methods, a direct clamping two-probe approach is proposed. Unlike the former two-probe method [13], the proposed method uses direct clamp-on type current probes and therefore there is no direct electrical contact to the power line wires between the LISN and the SMPS. Hence, it eliminates the needs of the coupling capacitors. Also, no isolating chokes are needed, making the measurement setup very simple to implement. With the vector network analyzer as a measurement instrument, both the magnitude and the phase information can be extracted directly without further processing. The proposed method is also highly accurate as it has the capability to eliminate the error introduced by the measurement setup.

The assumption underlying our extraction procedure is, that the input impedance of the SMPS behaves linearly. This is reasonably true, since -according to [11]- the “on” state impedance prevails during operation, and the impedance probing is done by means of small-signal perturbations, thus allowing linearization [14]. With the known impedance information, the design limita-

tions of previously mentioned methods can be overcome and a systematic EMI filter configuration to achieve the desired filter insertion loss performance becomes possible.

## II. Theory of the Direct Clamping Two-Probe Measurement

Two-probe measurement technique was first applied to measure the impedance of the equipment under test (EUT), e.g. operating small ac motor, fluorescent light, etc., within frequency range from 20 kHz to 30 MHz by [15]. Then, the power line impedance was measured within frequency range from 10 kHz to 32 MHz by [16] and 20 kHz to 30 MHz [17]. Later, the frequency range of power line impedance measurement is extended up to 500 MHz [18]. With the same concept, the characterizations of the DM and CM noise source impedances of the SMPS can be extracted as proposed in [13], [19] - [20].

The basic concept of the direct clamping two-probe method to measure any unknown impedance is illustrated in Fig. 1. It consists of an injecting current probe, a receiving current probe and a vector network analyzer (VNA). Port 1 of the VNA generates an AC signal into the closed loop through the injecting probe and the resulting signal current in the loop is measured at port 2 of the VNA through the receiving probe.

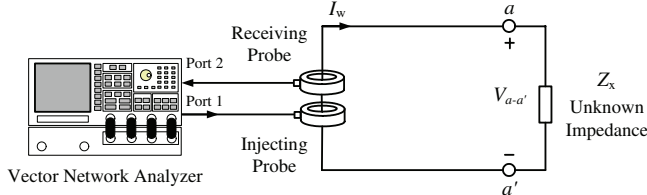


Fig. 1: Conceptual direct clamping two-probe measurement.

Fig. 2 shows the complete equivalent circuit of the measurement setup shown in Fig. 1 where  $V_1$  is the output signal source voltage of port 1 connected to the injecting probe and  $V_{p2}$  is the resultant signal voltage measured at port 2 with the receiving probe. The output impedance of port 1 and the input impedance of port 2 of the VNA are both  $50 \Omega$ .  $L_1$  and  $L_2$  are the primary inductances of the injecting and the receiving probes, respectively.  $L_w$  and  $r_w$  are the inductance and the resistance of the wiring connection that formed the circuit loop, respectively.  $M_1$  is the mutual inductance between the injecting probe and the circuit loop and  $M_2$  is the mutual inductance between the receiving probe and the circuit loop.  $Z_{p1}$  and  $Z_{p2}$  are the input impedances of the injecting and receiving probes, respectively.

The exciting signal source  $V_1$  induces a signal current  $I_w$  in the circuit loop through the injecting probe. From Fig. 2, three circuit equations result as follows:

$$\begin{bmatrix} V_1 \\ 0 \\ -V_{a-a'} \end{bmatrix} = \begin{bmatrix} 50 \Omega + Z_{p1} & 0 & -j\omega M_1 \\ 0 & 50 \Omega + Z_{p2} & +j\omega M_2 \\ -j\omega M_1 & +j\omega M_2 & r_w + j\omega L_w \end{bmatrix} \begin{bmatrix} I_1 \\ I_2 \\ I_w \end{bmatrix}. \quad (1)$$

Eliminating  $I_1$  and  $I_2$  from (1) gives

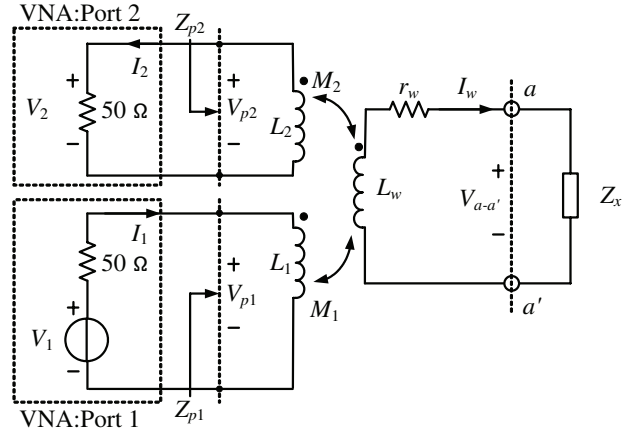


Fig. 2: Equivalent circuit of the two-probe measurement setup of Fig. 1.

$$V_{M1} = V_{a-a'} + (Z_{M1} + Z_{M2} + r_w + j\omega L_w)I_w, \quad (2)$$

where  $Z_{M1} = \frac{(\omega M_1)^2}{50 \Omega + Z_{p1}}$ ,  $Z_{M2} = \frac{(\omega M_2)^2}{50 \Omega + Z_{p2}}$  and  $V_{M1} = V_1 \left( \frac{j\omega M_1}{50 \Omega + Z_{p1}} \right)$ .

According to expression (2), the injecting probe can be reflected in the closed circuit loop as an equivalent current-controlled voltage source  $V_{M1}$  in series with a reflected impedance  $Z_{M1}$  and the receiving probe can be reflected in the same loop as another impedance  $Z_{M2}$ , as shown in Fig. 3. For frequencies below 30 MHz, the dimension of the coupling circuit loop is electrically small as compared to the wavelengths concerned. Therefore, the current distribution in the coupling circuit is uniform throughout the loop and  $V_{M1}$  can be rewritten as

$$\begin{aligned} V_{M1} &= (Z_{M1} + Z_{M2} + r_w + j\omega L_w + Z_x)I_w, \\ &= (Z_{setup} + Z_x)I_w. \end{aligned} \quad (3)$$

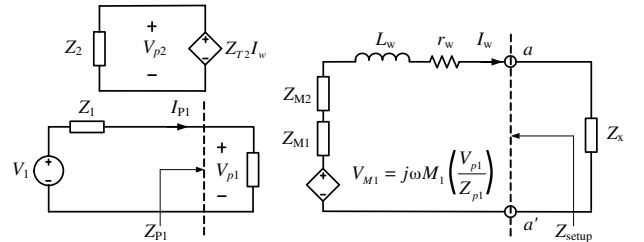


Fig. 3: Final equivalent circuit of the circuit loop connecting to the unknown impedance.

The equivalent circuit seen at a-a' by the unknown impedance  $Z_x$  can be substituted by an equivalent current-controlled voltage source  $V_{M1}$  in series with an impedance due to the measurement setup  $Z_{setup}$ . From (3),  $Z_x$  can be determined by

$$Z_x = \frac{V_{M1}}{I_w} - Z_{setup}. \quad (4)$$

The current  $I_w$  measured by the receiving probe is, according to the receiving probe loop of Fig. 3:

$$I_w = \frac{V_{p2}}{Z_{T2}}, \quad (5)$$

where  $V_{p2}$  is the signal voltage measured at port 2 of the VNA and  $Z_{T2}$  is the calibrated transfer impedance of the receiving probe

provided by the probe manufacturer. Substituting  $V_{M1}$  and (5) into (4) yields

$$Z_x = \left( \frac{j\omega M_1 Z_{T2}}{50 \Omega + Z_{p1}} \right) \left( \frac{V_1}{V_{p2}} \right) - Z_{setup}. \quad (6)$$

The excitation source  $V_1$  of port 1 of the VNA and the resultant voltage at the injecting probe  $V_{p1}$  is related by

$$V_1 = \left( \frac{50 \Omega + Z_{p1}}{Z_{p1}} \right) V_{p1}. \quad (7)$$

Substituting (7) into (6), the unknown impedance can finally be expressed as

$$Z_x = K \left( \frac{V_{p1}}{V_{p2}} \right) - Z_{setup}, \quad (8)$$

where  $K = \left( \frac{j\omega M_1 Z_{T2}}{Z_{p1}} \right)$ , which is a frequency dependent

coefficient. The ratio  $V_{p1}/V_{p2}$  can be obtained through the S-parameters measurement using the VNA. From Fig. 2, the resultant signal voltage source can be defined by  $V_{p1} = (S_{11}+1)V_{p1}+$  and the resultant measured voltage can be defined by  $V_{p2} = S_{21}V_{p1}+$  [18], [21]. As a result, the ratio of the two probe voltages is given by

$$\frac{V_{p1}}{V_{p2}} = \frac{S_{11} + 1}{S_{21}}, \quad (9)$$

where

$S_{11}$  = the measured reflection coefficient at port 1,

$S_{21}$  = the measured forward transmission coefficient at port 2.

The coefficient  $K$  and the setup impedance  $Z_{setup}$  can be obtained by the following steps. Firstly, measure  $V_{p1}/V_{p2}$  by replacing impedance  $Z_x$  with a known precision standard resistor  $R_{std}$ . As a rule of thumb, the resistance of  $R_{std}$  should be chosen somewhere in a middle range of measuring unknown impedance to be measured. Then, measure  $V_{p1}/V_{p2}$  again by short-circuiting a – a'. With these two measurements and (8), two equations (10) - (11) with two unknowns  $K$  and  $Z_{setup}$  are resulted. Hence,  $K$  and  $Z_{setup}$  can be obtained by solving (10) and (11). Once  $K$  and  $Z_{setup}$  are found, the two-probe setup is ready to measure any unknown impedance using (8).

$$R_{std} = K \left( \frac{V_{p1}}{V_{p2}} \right) |_{Z_x=R_{std}} - Z_{setup}, \quad (10)$$

$$0 = K \left( \frac{V_{p1}}{V_{p2}} \right) |_{Z_x=short} - Z_{setup}. \quad (11)$$

It is ought to be noted that, for the sake of clarity, Fig. 1 is oversimplified and does not contain the LISN powering the active device under test (the SMPS, in our case). The LISN impedance should be considered a part of  $Z_{setup}$ , without limitations. An additional remark is, that the injected signal of the VNA must be much larger than the background noise generated by the device under test in the frequency range of interest, so that the background noise does not alter the  $Z_x$  value, superimposing on the measured quantities. For most low and medium power active systems, such a condition can usually be met. However, if the active system is characterized by very high power and generates significant background noise, one could add a power amplifier at the output of port 1 of the VNA to increase the power of the injected signal, so that the said condition could be fulfilled.

### III. Measurement of Termination Impedances of the LISN

According to CISPR standard, the SMPS is normally powered through the LISN to ensure stable and repeatable AC mains impedance. Thus, in order to extract the noise source impedances, the termination impedances of the LISN must be determined beforehand. The DM as well as the CM output impedances of a LISN (Electro-Metrics MIL 5-25/2) are measured using the proposed method and the HP4396B impedance analyzer (100 kHz - 1.8 GHz). The measured DM impedance ( $Z_{LISN,DM}$ ) and the measured CM impedance ( $Z_{LISN,CM}$ ) of the LISN using both methods are compared to validate the measured results by proposed technique.

Using the two-probe method, the LISN can be measured with the AC power applied. However, the measurement using the impedance analyzer can only be made with no AC power applied to the LISN to prevent damage to the measuring equipment. For the two-probe method, AC power is applied to the input of the LISN and one or two 1  $\mu$ F "X class" capacitors are connected at the output of the LISN to implement an AC short circuit. It should be noted that because the impedance of 1  $\mu$ F capacitor is very low at measured frequency range, its impedance is not taken into account. A 1  $\mu$ F capacitor is connected between line-to-neutral for DM measurement. For CM measurement, two 1  $\mu$ F capacitors are needed, one connected between line-and-ground and another connected between neutral-and-ground. For the DM output impedance measurement, the line wire is treated as one single outgoing conductor and the neutral wire is treated as the returning conductor. In the case of CM measurement, the line and the neutral wires are treated as one single outgoing conductor, and the safety ground wire is treated as the returning conductor. The length of the connecting wire between the LISN and capacitor is chosen to be as short as possible to eliminate the parasitic inductance of the connecting wires.

However, since the connecting wire is different from the case of the simple resistor measurements, the  $Z_{setup,DM}$ ,  $Z_{setup,CM}$  and the frequency dependent coefficient ( $K_{DM}$  and  $K_{CM}$ ) need to be re-calibrated. For DM impedance measurement, the injecting and receiving probes are clamped on the connecting line wire only. The  $Z_{setup,DM}$  and  $K_{DM}$  can be obtained by measuring  $V_{p1}/V_{p2}$  when both LISN and "X class" capacitors are removed and short-circuiting the line and neutral wires at both ends. Again, measure  $V_{p1}/V_{p2}$  by connecting the precision standard resistor  $R_{std}$  ( $620 \Omega \pm 1\%$ ) at one end. For the CM impedance measurement, since the line and the neutral wires are treated as one single outgoing conductor, both current probes are clamped onto the line and the neutral wires. The  $Z_{setup,CM}$  and  $K_{CM}$  can be obtained by removing both LISN and two "X class" capacitors and measuring  $V_{p1}/V_{p2}$  when the line, neutral and ground wires are shorted at both ends. Then, measure  $V_{p1}/V_{p2}$  by connecting the precision standard resistor  $R_{std}$  ( $620 \Omega \pm 1\%$ ) between line-neutral and ground at one end. Substituting those measurement results into equations (10) and (11), the  $Z_{setup,DM}$ ,  $Z_{setup,CM}$  and the frequency dependent coefficients  $K_{DM}$  and  $K_{CM}$  can be obtained.

Moreover, since the LISN schematics and component values are provided by the manufacturers or standards, the DM and CM impedances of the LISN can be readily calculated. For comparison purposes, the simulated DM and CM impedances of the LISN ( $Z_{LISN,DM(simul.)}$  and  $Z_{LISN,CM(simul.)}$ ) using the datasheet provided by

manufacturer are also plotted as shown in Figs. 4 (a) - (b) and Figs. 5 (a) - (b), respectively. The comparisons of measured output impedance of LISN using the direct clamping two-probe approach ( $Z_{LISN,DM(2probes)}$  and  $Z_{LISN,CM(2probes)}$ ) and using the impedance analyzer ( $Z_{LISN,DM(IA)}$  and  $Z_{LISN,CM(IA)}$ ) are given in Fig. 4 and Fig. 5, respectively.

#### IV. Measurement of Noise Source Impedances of the SMPS

The measurement setups to extract the DM noise source impedance ( $Z_{SMPS,DM}$ ) and the CM noise source impedance ( $Z_{SMPS,CM}$ ) of a SMPS are shown in Figs. 6 (a) and (b), respectively. The model and technical specifications of the SMPS are: VTM22WB, 15 W, +12 Vdc/0.75 A, -12 Vdc/0.5 A. The SMPS is powered through the LISN (MIL 5-25/2). A resistive load is connected at the output of the SMPS for loading purposes. The DM impedance ( $Z_{LISN,DM}$ ) and the CM impedance ( $Z_{LISN,CM}$ ) of the LISN have been measured earlier in Section III and presented in Fig. 4 and Fig. 5, respectively.

According to the measurement procedure of Section II, we need first to extract the DM and the CM setup impedances,  $Z_{setup,DM}$  and  $Z_{setup,CM}$ , and the frequency dependent coefficients  $K_{DM}$  and  $K_{CM}$  of the measurement setup. For DM impedance measurement calibration process, the injecting and receiving probes are clamped on the connecting line and neutral wires as shown in Fig. 6 (a). The  $Z_{setup,DM}$  and  $K_{DM}$  can be obtained by measuring  $V_{p1}/V_{p2}$  when both LISN and SMPS are removed and short-circuiting the line and neutral wires at both ends. Again, measure  $V_{p1}/V_{p2}$  by connecting the precision standard resistor  $R_{std}$  ( $620 \Omega \pm 1\%$ ) at one end. For the CM impedance measurement calibration process, both current probes are clamped onto the line and the neutral wires, as shown in Fig. 6 (b). The  $Z_{setup,CM}$  and  $K_{CM}$  can be obtained by removing both LISN and SMPS and measuring  $V_{p1}/V_{p2}$  when the line, neutral and ground wires are shorted at both ends. Then, measure  $V_{p1}/V_{p2}$  by connecting the precision standard resistor  $R_{std}$  ( $620 \Omega \pm 1\%$ ) between line-neutral and ground at one end. Substituting those measurement results into equations (10) and (11), the  $Z_{setup,DM}$ ,  $Z_{setup,CM}$  and the frequency dependent coefficients  $K_{DM}$  and  $K_{CM}$  can be obtained. The transmission line effect of the wire connection can be ignored as the length of connecting wires ( $l$ ) from the LISN to the SMPS is 70 cm, which is much shorter than the wavelength of the highest frequency of interest (30 MHz). The measured impedances are the total impedances in the circuit loops and we designate  $Z_{T,DM}$  and  $Z_{T,CM}$  as the total DM and CM impedances of the circuit loops connecting the SMPS and LISN under AC powered up operating conditions. As a result,  $Z_{T,DM}$  and  $Z_{T,CM}$  are defined by

$$Z_{T,DM} = Z_{LISN,DM} + Z_{SMPS,DM} + Z_{setup,DM} \quad (12)$$

$$Z_{T,CM} = Z_{LISN,CM} + Z_{SMPS,CM} + Z_{setup,CM} \quad (13)$$

where

$$Z_{LISN,DM} = \text{DM output impedance of the LISN } [\Omega],$$

$$Z_{LISN,CM} = \text{CM output impedance of the LISN } [\Omega],$$

$$Z_{SMPS,DM} = \text{DM input impedance of the SMPS } [\Omega],$$

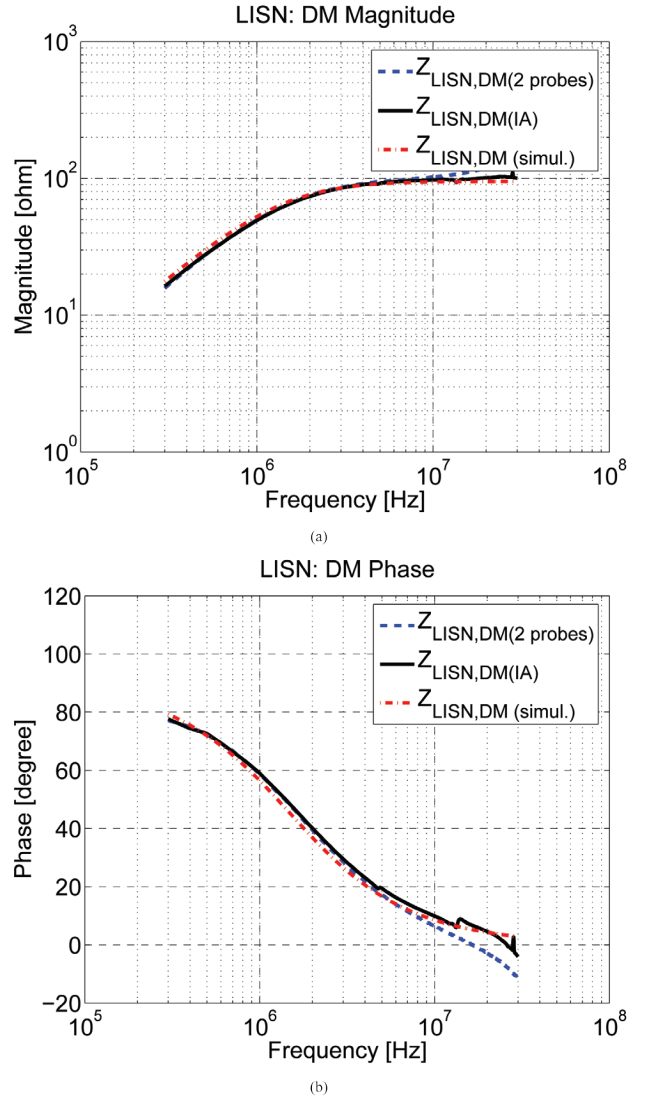


Fig. 4: Comparison of measured results for LISN. (a) DM magnitude; (b) DM phase.

$$Z_{SMPS,CM} = \text{CM input impedance of the SMPS } [\Omega],$$

$$Z_{setup,DM} = \text{DM impedance due to the measurement setup } [\Omega],$$

$$Z_{setup,CM} = \text{CM impedance due to the measurement setup } [\Omega].$$

With known  $Z_{LISN,DM}$ ,  $Z_{LISN,CM}$ ,  $Z_{setup,DM}$  and  $Z_{setup,CM}$ , once  $Z_T$  is measured, the DM and CM noise source impedances of the SMPS can be evaluated easily using (14) and (15), respectively.

$$Z_{SMPS,DM} = Z_{T,DM} - Z_{LISN,DM} - Z_{setup,DM}, \quad (14)$$

$$Z_{SMPS,CM} = Z_{T,CM} - Z_{LISN,CM} - Z_{setup,CM}. \quad (15)$$

Figs. 7 (a) and (b) show the magnitude and the phase of the extracted DM noise source impedance ( $Z_{SMPS,DM}$ ) in the frequency range from 300 kHz to 30 MHz. In general, the DM noise source impedance is dominated by the series inductive and resistive components at low frequencies; above 10 MHz, the effect of the diode junction capacitance of the full-wave rectifier begins to play a role. Figs. 8 (a) and (b) show the magnitude and the phase of the extracted CM



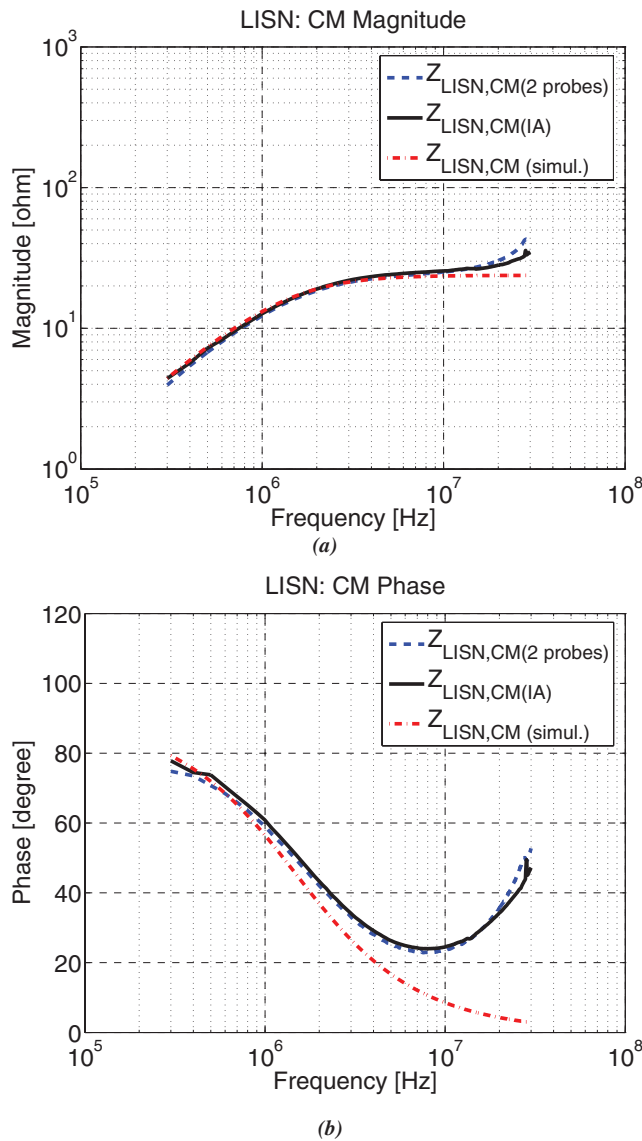


Fig. 5: Comparison of measured results for LISN. (a) CM magnitude; (b) CM phase.

noise source impedance ( $Z_{SMPS,CM}$ ). The CM noise source impedance is dominated by the effect of the parasitic capacitances of the SMPS e.g. the heat sink-to-ground parasitic capacitance.

## V. Comparison Between the SMPS and LISN Impedances

To sum up, the practical DM and CM impedance measurements of SMPS and LISN using the direct clamping two-probe method are concluded as follows:

- 1) *Pre-measurement calibration process*: The setup impedances ( $Z_{setup,DM}$  and  $Z_{setup,CM}$ ) and the frequency-dependent coefficients ( $K_{DM}$  and  $K_{CM}$ ) of the measurement setups must be determined according to the procedure outlined in Section III. Once these parameters are known, the measurement setup is ready to measure any unknown impedance using equation (8).
- 2) *Measurement of the noise termination impedances ( $Z_{LISN,DM}$  and  $Z_{LISN,CM}$ )*: As the SMPS is powered through the LISN, the LISN acts as

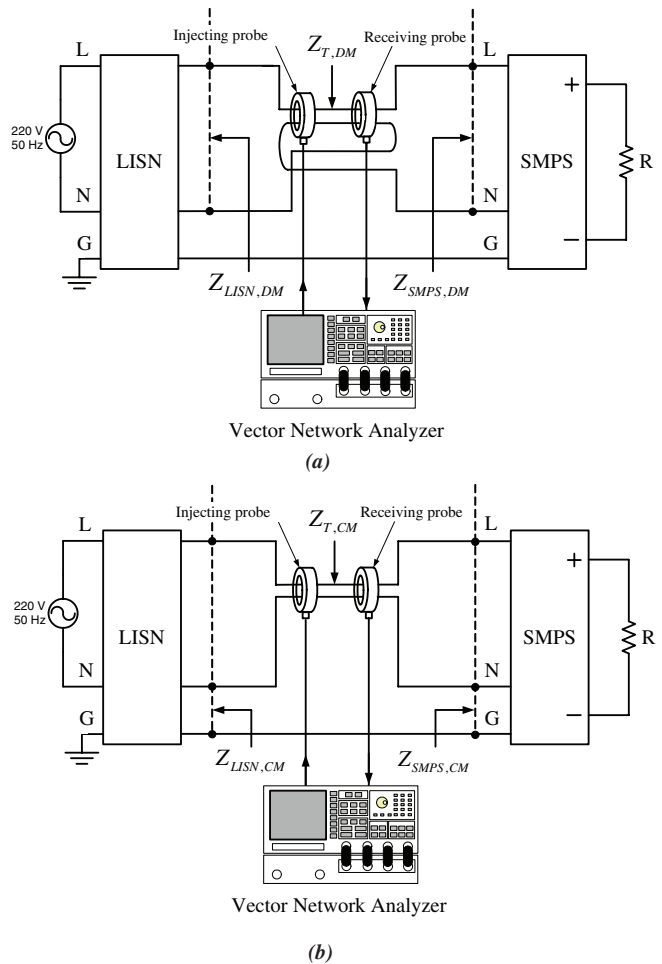


Fig. 6: Noise source impedance measurement setup of the SMPS. (a) DM; (b) CM.

a termination for the SMPS noise. To measure the LISN impedance, the SMPS in Fig. 6 (a) and (b) will be replaced by a capacitor, which serves as an AC short at high frequency. In the DM measurement setup, a  $1\ \mu\text{F}$  capacitor is connected between line and neutral. In the CM measurement setup, a  $1\ \mu\text{F}$  capacitor is connected between line and ground (nodes L and G) and another  $1\ \mu\text{F}$  capacitor is connected between neutral and ground (nodes N and G). The DM and CM impedances of the LISN can be determined by means of equation (8).

- 3) *Measurement of the noise source impedances ( $Z_{SMPS,DM}$  and  $Z_{SMPS,CM}$ )*: In Figs. 6 (a) and (b), the measured impedance using the two-probe setup is the total impedance in the circuit loop; we designate as  $Z_{T,DM}$  and  $Z_{T,CM}$  such measured impedances. With the known setup impedance obtained from Step 1 and the known LISN impedance from Step 2, the respective DM and CM impedances of the noise source (SMPS) can be found according to (14) and (15).

As an example, a SMPS (VTM22WB, 15W, +12VDC/0.75A, 12VDC/0.5A) is powered through a LISN (Electro-Metrics MIL 5-25/2) and characterized by means of the setups shown in Figs. 6 (a) and (b). The DM and CM impedances of the LISN (noise termination) and the SMPS (noise source) are determined with Steps 1 to 3 described earlier.

Figs. 9 (a) and (b) show the magnitudes and phases of the measured LISN and SMPS impedances in DM, respectively. Figs. 10 (a) and (b)

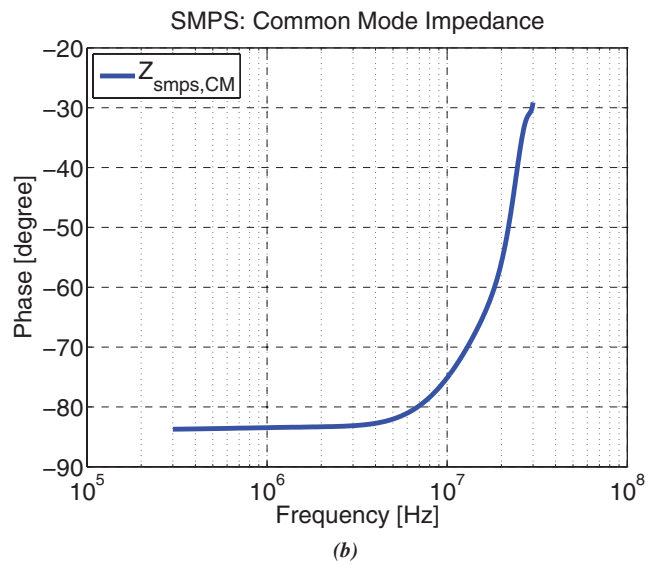
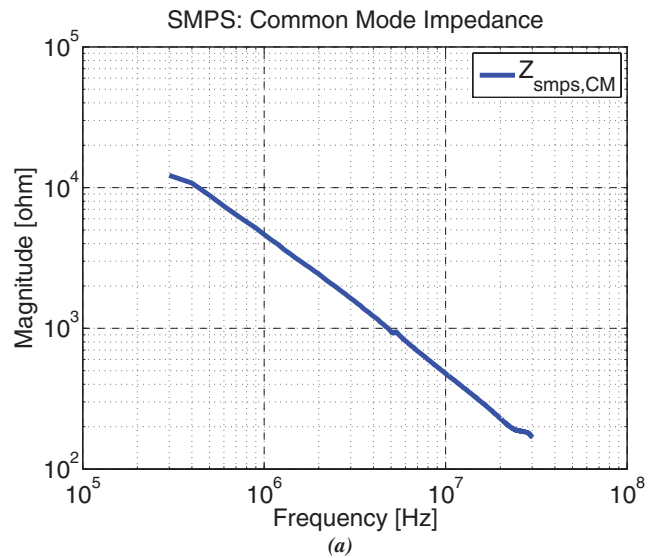
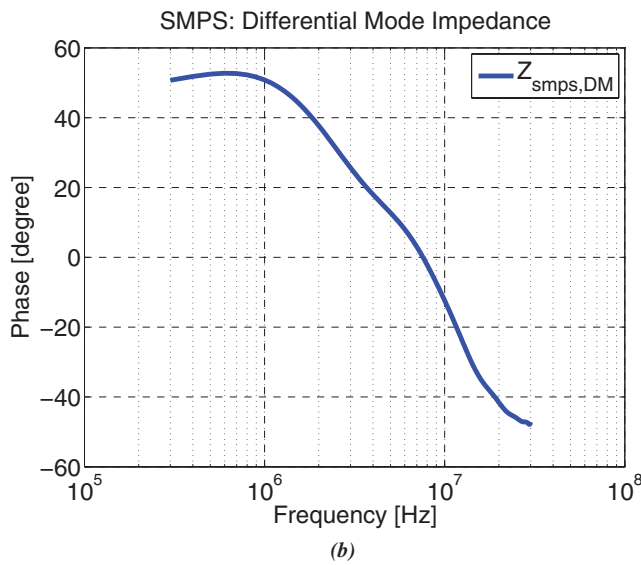
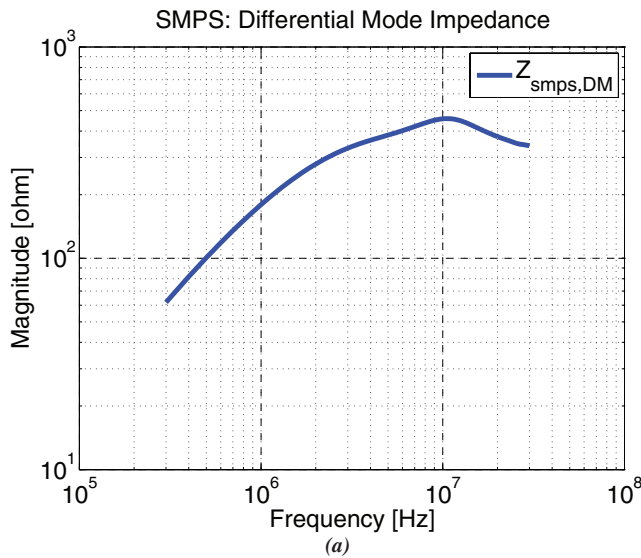


Fig. 7: Noise source impedance measurement. (a) DM Magnitude; (b) DM Phase.

Fig. 8: Noise source impedance measurement. (a) CM Magnitude; (b) CM Phase.

show the magnitudes and phases of the measured LISN and SMPS impedances in CM. From Fig. 9 (a) and (b), the DM SMPS impedance magnitude is higher than the DM LISN impedance by a few tens ohms to a few hundred ohms and their phases are spanning approximately 90 degrees, over the frequency range of measurements. Fig. 10 (a) and (b) show that the CM SMPS impedance is capacitive and rather regular over the frequency range of measurements, while the CM LISN impedance shows a phase change not easily explainable in terms of elementary circuit elements. With the known magnitudes and phases of the noise source (SMPS) impedance, noise termination (LISN) impedance, a systematic design of an EMI filter to meet a specific conducted EMI limit becomes possible.

## VI. Conclusion

For the noise source impedance extractions, a direct clamping two-probe approach is proposed to extract both amplitude and phase of DM and CM impedances of the termination load impedance i.e. line impedance stabilization network (LISN) and noise

source i.e. switched-mode power supply (SMPS) under actual operating conditions with a good accuracy. The proposed approach is very simple to implement, does not require modifications of the device under measurement, and provides both magnitude and phase of the tested impedance. for the noise source impedance extractions, a direct clamping approach is proposed, employing two probes to extract both amplitude and phase of DM and CM impedances of the LISN and SMPS under actual operating conditions with a good accuracy. The advantages of the proposed method can be concluded as follows.

- The unknown impedances of the system under test can be extracted without any modification of the system.
- Unlike the impedance analyzer, this approach is not limited to measure the unknown impedances under power off condition. The measuring unknown impedances might be either powered or not.
- The amplitude and phase of the DM and CM input impedances of a SMPS (noise source impedances) and the DM

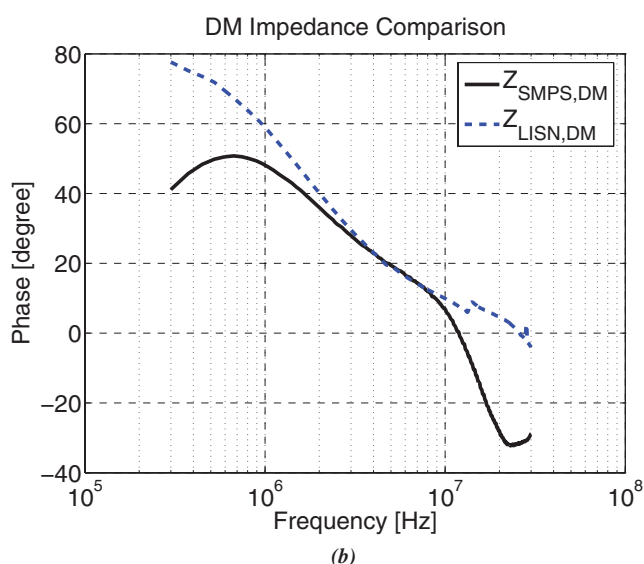
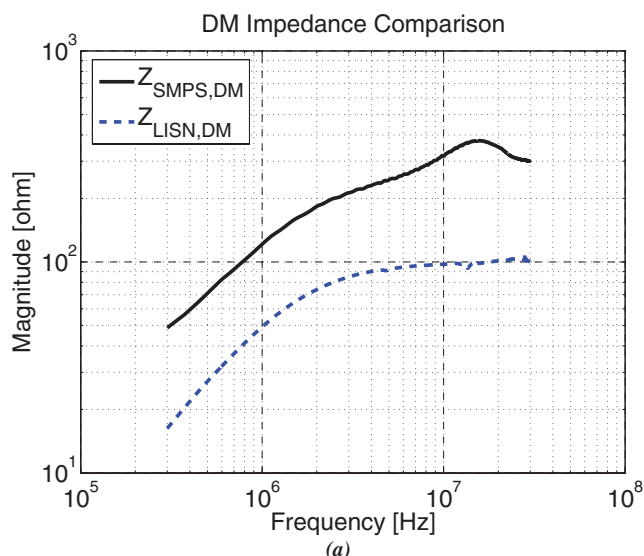


Fig. 9: Comparison of LISN and SMPS impedances. (a) DM Magnitude; (b) DM Phase.

and CM output impedances of LISN (load impedances) under their actual operating conditions can be extracted with high accuracy.

However, like any other measurement methods, the proposed method has some limitations which can be addressed as follows.

- For the results to be valid, it requires the condition where the injected signal is much higher than background noise. For very high power active systems, additional power amplifier may be necessary to meet the said condition.
- The accuracy of the proposed method can be ruined if the pre-measurement calibration process is not properly set. For example, any connecting wire loops must be made as small as possible to avoid any loop resonances below 30 MHz.
- To extract only the SMPS impedance, the power interconnection between LISN and SMPS must be as short as possible and is much shorter than the wavelength of the highest

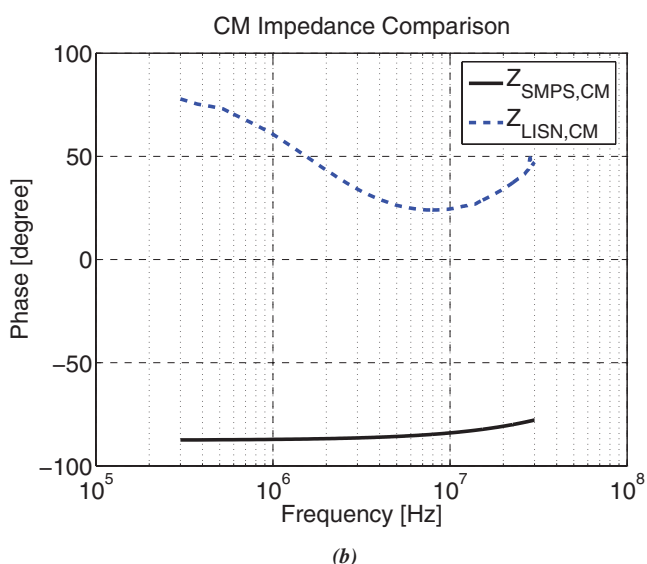
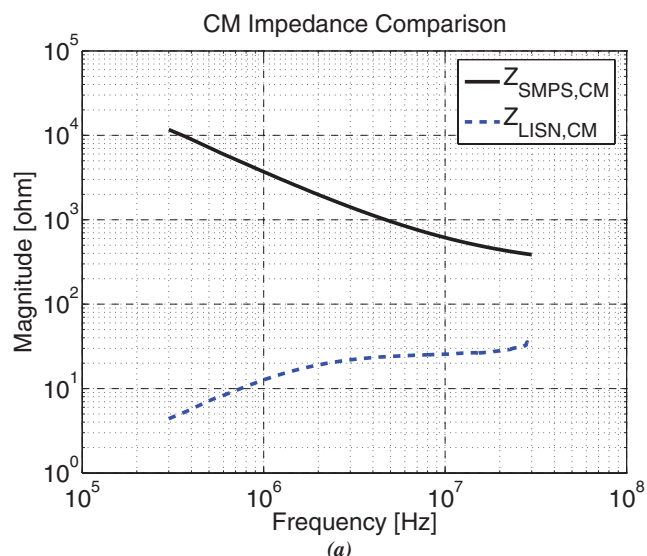


Fig. 10: Comparison of LISN and SMPS impedances. (a) CM Magnitude; (b) CM Phase.

frequency of interest (30 MHz) to minimize any transmission line effects.

- The range of the unknown impedances under measurement must be roughly known so that the precision resistor  $R_{std}$  can be chosen properly. The  $R_{std}$  must be chosen somewhere in the middle of the range of unknown impedance to be measured.

In the final paper of three-part series, a systematic EMI filter design based on information from direct clamping two-probe approach will be validated and demonstrated by various practical design examples.

## VII. Acknowledgment

The author would like to acknowledge useful suggestions and comments from Assoc. Prof. See Kye Yak and Prof. Flavio G. Canavero on the content of these series of articles.



## References

- [1] Clayton R. Paul, *Introduction to Electromagnetic Compatibility*, John Wiley & Sons, second edition, 2006.
- [2] L. Tihanyi, *Electromagnetic Compatibility in Power Electronics*, IEEE Press, 1997.
- [3] B. Garry and R. Nelson, "Effect of impedance and frequency variation on insertion loss for a typical power line filter," in 1998 *Proc. IEEE EMC Symposium*, pp. 691–695.
- [4] *Specification for Radio Disturbance and Immunity Measuring Apparatus and Methods Part 1: Radio Disturbance and Immunity Measuring Apparatus*, CISPR 16-1, 1999.
- [5] J. A. Ferreira, P. R. Willcock and S. R. Holm, "Sources, paths and traps of conducted EMI in switch mode circuits," in *Proc. 1997 IEEE Industry Applications Conf.*, pp. 1584–1591.
- [6] A. Guerra, F. Maddaleno and M. Soldano, "Effects of diode recovery characteristics on electromagnetic noise in PFCs," in *Proc. 1998 IEEE Applied Power Electron. Conf.*, pp. 944–949.
- [7] Q. Liu, S. Wang, F. Wang, C. Baisden, and D. Boroyevich, "EMI suppression in voltage source converters by utilizing DC-link decoupling capacitors," *IEEE Trans. Power Electron.*, vol. 22, no. 4, pp. 1417–1428, Jul 2007.
- [8] J. C. Fluke, *Controlling conducted emission by design*, New York: Van Nostrand Reinhold, 1991.
- [9] L.M. Schneider, "Noise source equivalent circuit model for off-line converters and its use in input filter design," in 1983 *Proc. IEEE EMC Symposium*, pp. 167–175.
- [10] M. J. Nave, *Power Line Filter Design for Switched-Mode Power Supplies*, VNR, 1991.
- [11] D. Zhang, D.Y. Chen, M.J. Nave and D. Sable, "Measurement of noise source impedance of off-line converters," *IEEE Trans. Power Electron.*, vol. 15, no. 5, pp. 820–825, Sep 2000.
- [12] J. Meng, W. Ma, Q. Pan, J. Kang, L. Zhang, and Z. Zhao, "Identification of essential coupling path models for conducted EMI prediction in switching power converters," *IEEE Trans. Power Electron.*, vol. 21, no. 6, pp. 1795–1803, Nov 2006.
- [13] K.Y. See and J. Deng, "Measurement of noise source impedance of SMPS using a two probes approach," *IEEE Trans. Power Electron.*, vol. 19, no. 3, pp. 862–868, May 2004.
- [14] D. M. Mitchell, *DC-DC Switching Regulator Analysis*, McGraw-Hill, 1988, ch. 4.
- [15] J. L. Brooks, "A low frequency current probe system for making conducted noise power measurements," *IEEE Trans. Electromagn. Compat.*, vol. 7, no. 2, pp. 207–217, June 1965.
- [16] R.A. Southwick and W.C. Dolle, "Line impedance measuring instrumentation utilizing current probe coupling," *IEEE Trans. Electromagn. Compat.*, vol. EMC-13, no. 4, pp. 31–36, Nov 1971.
- [17] J. R. Nicholson and J. A. Malack, "RF Impedance of power lines and line impedance stabilization networks in conducted interference measurement," *IEEE Trans. Electromagn. Compat.*, vol. 15, no. 2, pp. 84–86, May 1973.
- [18] P. J. Kwasniok, M. D. Bui, A. J. Kozlowski and S. S. Stanislaw, "Technique for measurement of powerline impedances in the frequency range from 500 kHz to 500 MHz," *IEEE Trans. Electromagn. Compat.*, vol. 35, no. 1, pp. 87–90, Feb 1993.
- [19] V. Tarateeraseth, Hu Bo, K. Y. See and F. Canavero, "Accurate extraction of noise source impedance of SMPS under operating condition," *IEEE Trans. Power Electron.*, vol. 25, no. 1, pp. 111–117, Jan 2010.
- [20] V. Tarateeraseth, K. Y. See, F. Canavero and R.W.Y. Chang, "Systematic electromagnetic interference filter design based on information from in-circuit impedance measurement," *IEEE Trans. Electromagn. Compat.*, vol. 52, no. 3, pp. 588–598, Aug 2010.
- [21] David M. Pozar, *Microwave Engineering*, John Wiley & Sons, third edition, 2005.

## Biography



**Vuttipon Tarateeraseth** received the B. Eng. (second-class honors) and M. Eng. degree both in electrical engineering from King's Mongkut Institute of Technology Ladkrabang (KMITL), Thailand, and Ph.D. in electronics and communications engineering from Politecnico di Torino, Italy. Since 2011, he is a lecturer at Department of Electrical Engineering, Srinakharinwirot University, Thailand. From 2010-2011, he was a lecturer at College of Data Storage Innovation, KMITL. Prior to 2007, he worked as a head of environment testing laboratory at Delta Electronics (Thailand) for three years. He also worked as an EMC engineer for two years under the Joint Development of Teaching Materials to Improve EMC Skills of Academic Staff and Postgraduate Electronic Designers Project funded by the European Commission. His research interests are mainly in the fields of EMI reduction techniques, EMC/EMI modeling, EMC instruments and measurements and EMI filter design. He is the author or coauthor of more than 40 technical papers published in international journals and conference proceedings and one book chapter. **EMC**